MIT Open Access Articles

Complementary genomic approaches highlight the PI3K/ mTOR pathway as a common vulnerability in osteosarcoma

The MIT Faculty has made this article openly available. *Please share* how this access benefits you. Your story matters.

Massachusetts Institute of Technology

Complementary genomic approaches highlight the PI3K/mTOR pathway as a common vulnerability in osteosarcoma

Jennifer A. Perry[a,1], Adam Kiezun[b,1], Peter Tonzi[a], Eliezer M. Van Allen[b,c], Scott L. Carter[b], Sylvan C. Baca[b,c], Glenn S. Cowley[b], Ami S. Bhatt[b,c], Esther Rheinbay[b], Chandra Sekhar Pedamallu[b,c], Elena Helman[b,c], Amaro Taylor-Weiner[b], Aaron McKenna[b], David S. DeLuca[b], Michael S. Lawrence[b], Lauren Ambrogio[b], Carrie Sougnez[b], Andrey Sivachenko[b], Loren D. Walensky[a,d], Nikhil Wagle[b,c,e], Jaume Mora[f], Carmen de Torres[f], Cinzia Lavarino[f], Simone Dos Santos Aguiar[g,h], Jose Andres Yunes[g,i], Silvia Regina Brandalise[g], Gabriela Elisa Mercado-Celis[j], Jorge Melendez-Zajgla[j], Rocío Cárdenas-Cardós[k], Liliana Velasco-Hidalgo[k], Charles W. M. Roberts[a,d], Levi A. Garraway[b,c,e], Carlos Rodriguez-Galindo[a,d], Stacey B. Gabriel[b], Eric S. Lander[b,l,m], Todd R. Golub[b,d,n], Stuart H. Orkin[a,d,n,2], Gad Getz[b,o,2,3], and Katherine A. Janeway[a,d,2,3]

[a]Department of Pediatric Oncology, Dana–Farber/Boston Children's Cancer and Blood Disorders Center, Boston, MA 02215; [b]The Broad Institute of MIT and Harvard, Cambridge, MA 02142; [c]Department of Medical Oncology, Dana–Farber Cancer Institute, Boston, MA 02215; [d]Department of Pediatrics, [e]Department of Medicine, [l]Department of Systems Biology, [o]Department of Pathology, Harvard Medical School, Boston, MA 02115; [f]Department of Pediatric Hematology and Oncology, Hospital Sant Joan de Déu, 08950 Barcelona, Spain; [g]Department of Pediatric Oncology, Centro Infantil Boldrini, Campinas, 13083-210, Brazil; [h]Center for Pediatric Research, [i]Medical Genetics Department, Faculty of Medical Sciences, State University of Campinas, Campinas 13083-887, Brazil; [j]Subdirection of Basic Research, National Institute of Genomic Medicine, 14610, Mexico City, Mexico; [k]Department of Oncology, National Institute of Pediatrics, 04530, Mexico City, Mexico; [m]Department of Biology, Massachusetts Institute of Technology, Cambridge, MA 02139; and [n]Howard Hughes Medical Institute, Chevy Chase, MD 20815

Contributed by Stuart H. Orkin, October 9, 2014 (sent for review July 25, 2014)

Osteosarcoma is the most common primary bone tumor, yet there have been no substantial advances in treatment or survival in three decades. We examined 59 tumor/normal pairs by whole-exome, whole-genome, and RNA-sequencing. Only the *TP53* gene was mutated at significant frequency across all samples. The mean nonsilent somatic mutation rate was 1.2 mutations per megabase, and there was a median of 230 somatic rearrangements per tumor. Complex chains of rearrangements and localized hypermutation were detected in almost all cases. Given the intertumor heterogeneity, the extent of genomic instability, and the difficulty in acquiring a large sample size in a rare tumor, we used several methods to identify genomic events contributing to osteosarcoma survival. Pathway analysis, a heuristic analytic algorithm, a comparative oncology approach, and an shRNA screen converged on the phosphatidylinositol 3-kinase/mammalian target of rapamycin (PI3K/mTOR) pathway as a central vulnerability for therapeutic exploitation in osteosarcoma. Osteosarcoma cell lines are responsive to pharmacologic and genetic inhibition of the PI3K/mTOR pathway both in vitro and in vivo.

osteosarcoma | TP53 | PI3K | mTOR | genomics

Osteosarcoma (OS), the most common primary bone tumor, is an aggressive cancer that affects children, adolescents, and young adults. In contrast to the improvements in 5-year overall survival for childhood cancers from 58% to 82% in the past three decades, the overall survival for pediatric OS has remained static over that same time period at 60% (1, 2).

Predisposition to OS is associated with germline syndromes, including hereditary retinoblastoma and Li-Fraumeni syndrome (3, 4). OS is also seen in syndromes with mutations in *RECQ* helicases and *SQSTM1* (5, 6). However, most cases of OS develop sporadically and are characterized by complex genomics. The first genome-wide association study conducted in OS only identified two susceptibility loci implicating one gene, *GRM4*, a glutamate receptor (7).

Linkage with hereditary retinoblastoma and Li Fraumeni led to the recognition of recurrent somatic alterations in *TP53*, *RB1*, and genes interacting with TP53 and RB1 in OS (8, 9). Candidate-gene approaches demonstrated recurrent somatic mutations, deletions, and rearrangement affecting *TP53* (9). Additional

mechanisms of p53 inactivation described in OS are *MDM2* and *COPS3* amplification (8, 9). *RB1* mutations are present in 6% and deletions or structural alterations are seen in 40% of cases (10, 11). *CDKN2A* is deleted in 10–20% of OS (9, 12). Multiple other cancer-associated genes have been reported to be altered in OS [reviewed in Kansara and Thomas (5)]. Many of these studies

Significance

We present, to our knowledge, the first comprehensive next-generation sequencing of osteosarcoma in combination with a functional genomic screen in a genetically defined mouse model of osteosarcoma. Our data provide a strong rationale for targeting the phosphatidylinositol 3-kinase/mammalian target of rapamycin pathway in osteosarcoma and a foundation for rational clinical trial design. These findings present an immediate clinical opportunity because multiple inhibitors of this pathway are currently in clinical trials.

investigating somatic alterations in specific genes were performed on small numbers of tumors with low-throughput techniques. More recently, next-generation sequencing of 34 osteosarcomas identified recurrent alterations in *ATRX* and *DLG2*, in addition to *TP53* and *RB1* (13). This next-generation sequencing study used in depth analysis of whole-genome sequence data and demonstrated that OS tumors have multiple rearrangements across the genome, kataegis, and a high degree of intratumor heterogeneity. Chromothripsis has been described in selected cases (14, 15). To date, none of these discoveries have led to the development of molecularly targeted therapies or improved survival for OS patients.

Because treatment for OS has not changed appreciably in the past 30 years, new approaches to treating the disease are imperative. We sought to identify tractable therapeutic targets in OS by performing next-generation sequencing and a comprehensive analysis of the genomic alterations in OS. We anticipated challenges in identifying a gene or genes altered in a large proportion of cases because of the difficulty collecting a large sample size in such a rare tumor, genomic complexity and heterogeneity. We hypothesized that we could identify genes or pathways required for OS survival by combining sequencing data with four methods for identifying essential genes, including: (*i*) pathway analysis, based on the mutational profile; (*ii*) a heuristic algorithm used to identify alterations with the potential to be clinically actionable; (*iii*) a comparative oncology approach using whole exome sequencing from a mouse model of OS; and (*iv*) a genome-wide functional shRNA screen in murine OS to identify essential genes. Taken together, the data implicate the phosphatidylinositol 3-kinase/mammalian target of rapamycin (PI3K/mTOR) pathway as a key target for the treatment of OS.

Results

Clinical and Sequence Data Characteristics. We examined OS tumor/normal (blood) sample pairs by whole-genome sequencing (WGS; 13 cases), whole-exome sequencing (WES; 59 cases), and RNA-Sequencing (RNASeq; 35 cases) (Fig. 1). Clinical features of the patient population including outcome were typical for OS, with the exception of a higher proportion (47%) with metastases at diagnosis (Fig. S1*A*). All cases except two were sporadic, and no patients had clinically apparent germline syndromes associated with OS.

WES of ~33 Mb of protein-coding sequence yielded a median of 103× tumor (range 60×–188×) and normal (range 56×–206×) depth of coverage. A median of 88.2% (range 84–91%) of exonic bases were powered for discovering mutations. WGS yielded a median of 36× tumor (range 30×–61×) tumor and 35× normal (range 27×–38×) depth of coverage. In WGS, a median of 89% of genomic bases (range 87–90%) were powered for discovering mutations. Bases were considered powered for discovering mutations if they were covered with at least 14 reads in the tumor sample and at least 8 reads in the normal sample. The thresholds were selected to achieve 80% power for mutations at an allelic fraction of 0.3 (16).

Deleterious Germline Variants in *TP53* Are Common in Osteosarcoma. We examined germline variants of the 59 normal samples by WES. Twenty rare nonsilent variants were present in nine candidate genes after excluding missense variants classified as "benign" by PolyPhen-2 (Table S1) (17). Variants present in more than two normal samples were detected in only two genes: *TP53* (*n* = 7) and *SQSTM1* (*n* = 4). Germline mutations in *TP53* were present at a higher frequency (12%) than previously reported (3%) (4). All seven *TP53* variants were previously reported. We also examined somatic loss of heterozygosity of the germline variant alleles and found that only *TP53* germline variants were subject to a "second hit" by loss of heterozygosity of the wild-type allele (Table S1). Four rare nonsilent nucleotide variants in *SQSTM1* were identified. Three of these were identical: p.K238E, a SNP (rs11548633) in the TRAF6 binding

domain, and p.A426V, a mutation previously linked to Paget's disease of bone (18).

Osteosarcoma Marked by High Mutation Rate and Kataegis. In the coding regions of the OS genomes (59 WES samples), we detected a median of 37 somatic, nonsilent mutations per case (range 7–237), corresponding to a median somatic mutation rate of 1.2 mutations per megabase. To better understand the mechanisms leading to mutations in OS, we examined the distribution and categories of somatic point mutations across the genome. We observed a prevalence of localized hypermutation, in particular involving closely spaced C > T and C > G mutations in TpCpX trinucleotide contexts in several samples. This phenomenon, termed kataegis, was recently described in breast cancer and, subsequently, OS (13, 19). Using "rainfall" plots of C > T and C > G mutations derived from WGS, we identified kataegis in 11 of 13 (85%) OS samples. As previously described, kataegis events overlapped with genomic rearrangements in OS (Fig. 2). Kataegis has been linked, in other diseases, to APOBEC family proteins, which play a role in innate antiviral defense (19). To test the hypothesis of viral involvement, we examined WGS, WES, and RNASeq data for the presence of viral nucleic acid sequences by PathSeq but did not detect any enrichment (20).

Osteosarcomas Exhibit Genomic Complexity and Heterogeneity. Copy number analysis using the WES data from 59 samples with GISTIC2 revealed 15 significant arm-level events, 15 significant focal amplifications, and 22 significant focal deletions (Fig. S1*B* and Datasets S1 and S2) (21). The observed focal copy number alterations in this study are consistent with previous reports. The most significant focal deletions included the genes *RB1*, *TP53*, and *CDKN2A/B* (9, 10, 12). The most significant focal amplifications were in the *COPS3*, *CCNE1*, *CDK4,* and *MYC* genes, and 6p12.3 amplifications (8, 22).

In the 13 WGS samples, a median of 230 (range 3–1,059) rearrangements per OS genome were observed, which is much higher than that seen in 275 TCGA (The Cancer Genome Atlas) tumor/normal WGS samples from other tumor types [median 48 (range 0–699), *P* < 3.5e-5, one-sided Mann–Whitney test] (23). No recurrent fusion events were found; however, rearrangements with breakpoints near *TP53* occurred with highest frequency among 2,586 genes (Dataset S3). Additionally, RNAseq data revealed that *TP53* was a recurrent fusion partner (3 of 35 samples) (Dataset S3). Integrative analysis of genomic breakpoints and copy number data were performed using the ChainFinder algorithm (24). Complex rearrangements indicative of chromoplexy were abundant in OS, and could be identified in samples both with high and low degrees of overall genomic rearrangement (25). We detected complex chains of rearrangements in 11 OS genomes (Fig. 2 and Dataset S4). The percentage of chromosomal breakpoints involved in a chain ranged from 27–70% (median 44%) across osteosarcomas. Chains of rearrangements from all tumors involved multiple chromosomes (median 4, range 3–6) and all but one involved multiple "deletion bridges" (median 6, range 0–29), which indicate large segments of DNA deletions at fusion junctions. Consistent with observations in other cancer types, regions of kataegis were highly correlated with copy number breakpoints and rearrangement sites.

OS samples are heterogeneous and highly complex. Among the 59 WES samples we analyzed, estimates of sample purity ranged from 19 to 100% (median 55%) and average cancer cell ploidy ranged from 1.42 to 4.31 (median 2.09). This finding is consistent with the massive complexity revealed by rearrangement analysis and points to frequent occurrence of genome doublings in OS: indeed, 12 of 55 (12.8%) samples for which ploidy estimations were obtained had ploidy above 3 (Dataset S5).
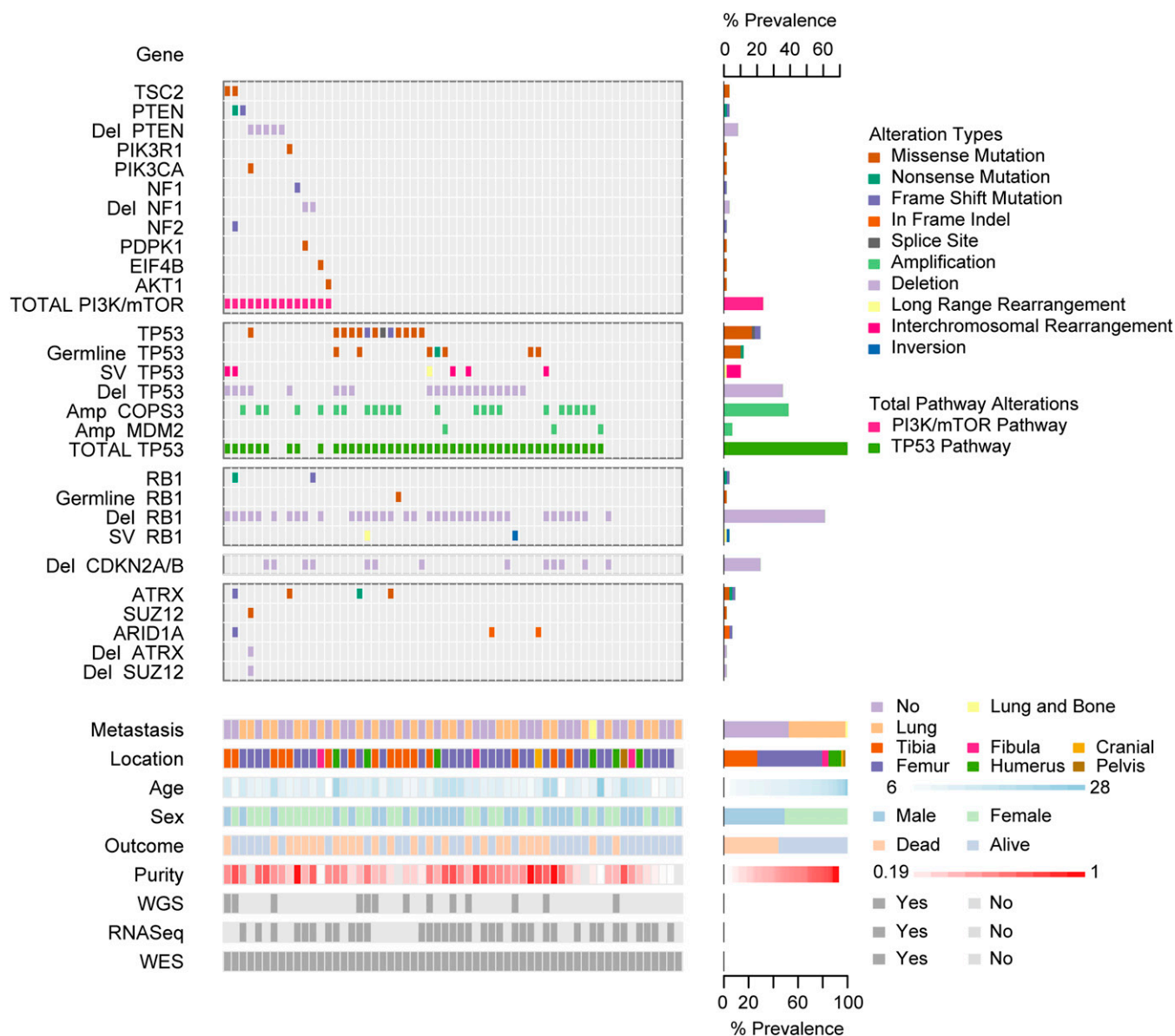
Fig. 1. Summary of sequencing results highlighting alterations in the PI3K/mTOR pathway, TP53, RB1, and TP53 and RB1 interacting genes, demographic and clinical variables, and sequencing characteristics. Each column represents a patient sample. The bottom section of the graph indicates the sequencing characteristics, demographic, and clinical data for each patient. The top section of the graph indicates the types of alteration for each gene or pathway per sample. Copy number alterations for PI3K/mTOR pathway genes, ATRX, SUZ12, and ARID1A were determined with the heuristic algorithm PHIAL. Copy number alterations for TP53, RB1, and TP53 and RB1 interacting genes were determined with GISTIC2. Amp, amplification; Del, deletion; SV, structural variation; long-range rearrangement, intrachromosomal rearrangements >1 Mb.

Frequent Alterations in *TP53* and *RB1* and in TP53 and RB1 Interacting Genes. Analysis of sequencing data using algorithms optimized for identifying recurrent events across samples identified a limited number of events, previously known to occur in OS. The MutSigCV (mutation significance) algorithm identified only one gene mutated at significant frequency across the 59 WES samples (at *q*-value threshold of 0.1): *TP53* (Fig. 1 and Dataset S6) (26). *TP53* was mutated in 22% of samples. 85% of the *TP53* mutations were missense or frameshift mutations in the DNA binding domain (Fig. S1C). Of the genes listed in the COSMIC database, the only other genes with nonsilent mutations occurring in more than one case were *RB1* and *PTEN* (27, accessed May, 2014).

We examined each sample for the presence of known mechanisms of *TP53* and *RB1* inactivation and for alterations in

known TP53 and RB1 interacting genes (Fig. 1). The results are summarized in Table 1. Fifty-six percent of cases had alterations resulting in both TP53 and RB1 inactivation. Inactivation of TP53 was observed in 75% of cases and surprisingly, 34% of cases have multiple mechanisms of TP53 inactivation. The types and relative frequency of genomic events in *TP53* and *RB1* are similar to prior reports (10, 11). Amplification of MDM2 and COPS3, proteins proposed to negatively regulate TP53 protein stability, were observed in 5% and 39% of cases, respectively (8, 9).

Alterations in PI3K/mTOR Pathway Genes Are Frequent in Osteosarcoma. To overcome difficulties in identifying significant common alterations in a tumor with high intra- and intertumor heterogeneity and relatively small sample size, we combined multiple analytical and genomic approaches to deepen the analysis.
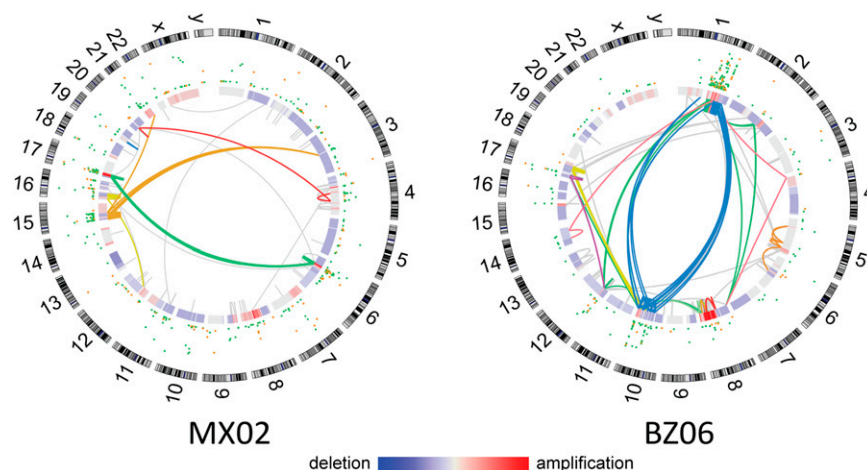
Fig. 2. Associations between chromosomal rearrangements and clustered single-nucleotide mutations are evident in osteosarcoma. Representative Circos plots are labeled with sample ID. Chromosomes are depicted on the outer most track. C > T (green) and C > G (yellow) mutations are plotted according to the distance to the nearest mutation from 1 bp (inner circle) to 5 kb (toward outside of circle). Blue-red heatmap track indicates whole-genome sequence-based copy number ratio estimates. Arcs represent rearrangements and are depicted in the same color if they are statistically unlikely to have occurred independently of one another, as assessed by ChainFinder.

First, we combined gene set enrichment analysis (GSEA) with mutational analysis and identified 32 pathways as being significantly affected by mutations across the 59 WES samples using the GSEA MSigDB Canonical Pathway collection ($q < 0.1$) (Dataset S7) (28, 29). Twenty-two pathways, including the 21 most significant pathways, contained *TP53* and are likely significant because of the frequency of mutations in this gene (*TP53* was the only significantly mutated gene across samples) (Fig. 3A). Of the remaining 10 significant pathways, 4 implicate the PI3K/mTOR signaling pathway: PTEN, IGF1/mTOR, RAS, and AKT (Fig. 3B). Four more pathways were statistically significant and contained members of the PI3K/mTOR signaling pathway but not *TP53*: IL2RB, RACCYCD, IL-7, and HCMV.

Pathway analysis indicated that the PI3K/mTOR pathway may be altered in OS, so we evaluated each genome individually with the objective of identifying mutations and copy number alterations in known cancer pathways, particularly those potentially inhibited with targeted therapies. To identify the most clinically relevant alterations in each sample, analysis of sequencing data and ranking of gene alterations by biologic and clinical relevance

was performed using the Precision Heuristics for Interpreting the Alteration Landscape (PHIAL) algorithm (Dataset S8) (30). Samples contained a range of one to five potentially actionable alterations. This method identified 24% of patients as having alterations in the PI3K/mTOR pathway (Fig. 1 and Table 2). There were five *PTEN* deletions, a *PTEN* nonsense mutation, and a *PTEN* frameshift mutation. There were two *TSC2* tuberin domain mutations, both previously reported to occur in individuals affected by tuberous sclerosis. There was an *NF1* frameshift mutation. A *PIK3CA* mutation at amino acid position 545, a mutation hotspot, was identified (27, accessed April 9, 2013). Mutations were identified in PI3K/mTOR pathway components *PDPK1*, *AKT1*, and *EIF4B* and are predicted to be damaging by PolyPhen-2 (31). For *PDPK1* and *AKT1*, mutations resulted in amino acid changes in key protein domains. The *PIK3R1* and one of the *EIF4B* mutations were not predicted to be damaging. In addition to PI3K/mTOR pathway alterations, PHIAL identified the presence of additional alterations, suggesting the potential for response to targeted agents (Table 2). The genes affected include *MYC*, growth factor receptor tyrosine kinases, Wnt pathway members, cell cycle regulatory molecules, and coordinators of DNA repair. In total, 20 of 59 patients (34%) had alterations with potential clinical implications. This method also identified alterations in epigenetic regulators *SUZ12*, *ATRX*, and *ARID1A* (Fig. 1).

Next, in a comparative oncology approach, we sequenced nine tumor/normal pairs (WES) from a mouse model of OS created via conditional deletion of *Tp53* and *Rb1* in the preosteoblast (Dataset S9) (32). Two PI3K/mTOR pathway genes were affected by somatic mutations in both mouse and human tumors: *PTEN* and *PIK3R1*. The *Pten* mutation in the murine tumor was a nonsense mutation p.Y16*. The *Pik3r1* missense mutation, p.S629N, lies within the C-terminal Src homology 2 domain, a region demonstrated to be affected by mutations in endometrial cancer (33).

Pik3ca and Mtor Are Essential for Osteosarcoma Proliferation and Survival. Finally, we performed a functional genomics screen to try to understand the relationship between the complicated genotype in OS and the functional dependencies in an unbiased fashion. To identify genes essential for the proliferation and survival of OS, we performed a genome-wide, pooled shRNA screen in a primary cell line derived from murine OS (mOS482) (Fig. 4A) (32). Cells were infected with a pool of 40,000 lentivirally delivered shRNAs, targeting ~8,400 genes (Dataset S10). The

Table 1. Frequent alterations in *TP53* and *RB1* and in TP53 and RB1 interacting genes in 59 osteosarcoma cases

Alteration	*n*	%
TP53 alterations		
TP53 mutation	13	22
TP53 rearrangement	8	14
TP53 deletion	21	39
COPS3 amplification	23	39
MDM2 amplification	3	5
One mechanism *TP53* inactivation	24	41
Multiple mechanisms *TP53* inactivation	20	34
Total *TP53* inactivation	44	75
RB1 alterations		
RB1 mutation	2	3
RB1 deletion	36	61
Combined *RB1* and *TP53* alterations		
Only *TP53* inactivation	11	19
Only *RB1* inactivation	4	7
Both *TP53* and *RB1* inactivation	33	56
Neither *RB1* nor *TP53* inactivation	11	19

A

B

Fig. 3. TP53 and PI3K/mTOR pathways are significantly mutated in osteosarcoma. GSEA combined with mutational analysis (MutSig2.0) identified 32 significantly mutated pathways (MSigDB Canonical Pathway gene sets) across 59 human osteosarcoma WES samples (q < 0.1). (A) Twenty-two pathways included the *TP53* gene and (B) eight pathways implicated the PI3K/mTOR pathway by inclusion of *PIK3CA* and/or *MTOR*, while excluding *TP53*.

relative abundance of each shRNA at the endpoint (18 doublings) relative to the initial reference pool was determined by massively parallel sequencing of the lentiviral DNA. Individual hairpins were rank ordered and RNAi gene enrichment (RIGER) analysis was used to collapse the normalized shRNA ranked list to gene rankings by two statistical methods: a weighted second best ($P \leq$

0.05) method and the Kolmogorov–Smirnov ($P \leq 0.05$) non-parametric rank statistic (Dataset S11 and S12). At the intersection were 172 genes. The 172 genes were enriched for cell cycle genes but also included *Pik3ca*, the α-catalytic subunit of PI3K, and *Mtor* (Fig. 4*B* and Dataset S13). shRNAs against these genes were inhibitory to mOS cell growth (mOS482 and mOS202) while having minimal effect on a noncancerous bone cell (Kusa4b10) (Fig. 4*C*) (34). To determine whether gene candidates identified in the in vitro screen were essential for OS proliferation and survival in vivo, we screened for shRNAs that become depleted upon OS formation in mice. A pool of shRNAs targeting *Pik3ca*, *Mtor*, and controls (four shRNAs per gene) was introduced into mOS482 cells that were then transplanted into recipient mice (Fig. S2*A*). Six weeks later, orthotopic tumors were isolated and massively parallel DNA sequencing was used to determine the abundance of each shRNA from tumors and preinjection cells. shRNAs against *Pik3ca* and *Mtor* were significantly depleted compared with control shRNAs (Fig. 4*D*). To confirm isoform specificity of PI3K's role in OS cell growth, three distinct mouse OS cell lines (mOS202, mOS482, and mOS493) were infected with shRNAs targeting *Pik3ca* or *Pik3cb* (Fig. S2*B*). Compared with both control and *Pik3cb* knockdown, *Pik3ca* knockdown caused growth arrest in mOS cells (Fig. 4*E*). Taken together, the in vitro and in vivo shRNA screen data indicate that OS cell line proliferation and tumor formation are dependent on the *Pik3ca* and *Mtor* genes.

PI3K/mTOR Inhibitors Suppress Osteosarcoma Proliferation. The occurrence of alterations in the PI3K/mTOR pathway in 24% of human OS samples and the identification of *Pik3ca* and *Mtor* in the murine OS genomic shRNA screen suggest that the PI3K/mTOR pathway is a potential unifying vulnerability to be exploited for targeted therapy in OS. Consequently, the PI3K/mTOR dual inhibitors GSK2126458 and BEZ235 and the PIK3CA-selective inhibitor PIK75 were tested against four human and three murine OS cell lines and MCF7 cells, a breast cancer cell line with a PIK3CA p.E545K mutation previously demonstrated to undergo

Table 2. PI3K/mTOR pathway alterations and other potentially actionable alterations identified in 20 osteosarcoma samples using the PHIAL algorithm

Gene	Alterations	*n*	Sample ID	Molecularly targeted agent
PI3K/mTOR pathway alterations				
TSC2	p.R611W, p.H593R	2	BZ04, BZ18	PI3K/mTOR inhibitor
PTEN	p.E288*, p.P244fs	2	BZ04, BZ09	PI3K/mTOR inhibitor
PTEN	Deleted	5	DF01, BZ03, SJD12, BZ06, SJD03	PI3K/mTOR inhibitor
PIK3CA	p.E545D	1	DF01	PI3K/mTOR inhibitor
AKT1	p.T443M	1	BZ29	AKT inhibitor
PIK3R1	p.P84L	1	SJD13	PI3K/mTOR inhibitor
PDPK1	p.G530E	1	BZ21	AKT inhibitor
EIF4B	p.R304K, p.R331K	1	SJD02	None
NF1	p.S2309fs	1	BZ14	PI3K/mTOR inhibitor
NF1	Deleted	2	BZ08, BZ21	PI3K/mTOR inhibitor
NF2	p.P170fs	1	BZ04	PI3K/mTOR inhibitor
Growth factor receptor tyrosine kinases				
PDGFRA	Amplified	1	DF01	Imatinib
PDGFRB	p.L803F	1	BZ19	Imatinib
JAK1	p.K245R, p.P548S	2	MX02, BZ11	Jak inhibitor
ALK	p.K911T, p.A585T	2	BZ33, BZ03	Crizotinib
KDR	p.S965R	1	BZ04	Pan-tyrosine kinase inhibitor
FGFR4	p.R171H	1	BZ30	FGFR inhibitor
Other				
CDKN2A/B	Deleted	2*	SJD12, BZ38	CDK4/6 inhibitor
GSK3B	p.S9F	1	BZ11	Wnt pathway inhibitor
ATM	Deleted	1	DF01	PARP inhibitor
MYC	Amplified	1	DF01	BET-bromodomain inhibitor

*Only samples with preserved *RB1* counted, because CDK inhibitors do not function in the absence of RB1 protein.
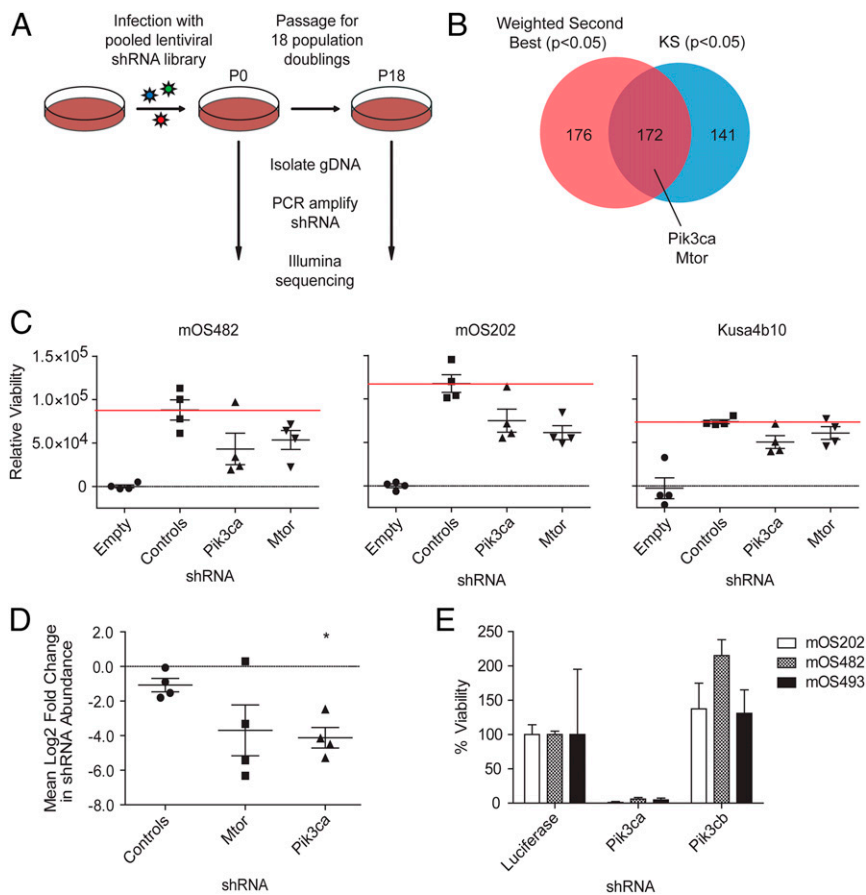
Fig. 4. PI3K/mTOR identified as essential by in vitro and in vivo functional genomics screening. (*A*) Schematic of experimental design of genome-wide shRNA screen in mouse osteosarcoma (mOS) cell line. (*B*) Venn diagram outlining the overlap of genes identified by two methods of analysis: weighted second best and Kolmogorov–Smirnov statistic in GENE-E/RIGER. (*C*) The relative viability of mOS cell lines, determined by Alamar Blue assay, expressing four individual shRNAs each targeting *Mtor*, *Pik3ca*, or control shRNAs (GFP, LacZ, Luciferase, and RFP) compared with uninfected cells that were puromycin selected for 8 d (empty). Horizontal bars represent mean and SEM, $n = 3$. (*D*) Mean log-twofold change in shRNA abundance of control (GFP, LacZ, Luciferase, and RFP) or experimental shRNAs from five tumor samples compared with preinjection samples. *$P < 0.01$. (*E*) The relative viability of mOS cell lines expressing shRNAs targeting either *Pik3ca*, *Pik3cb*, or control (luciferase) at 9 d postinfection and puromycin selection determined by WST-1assay. Error bars are SEM, $n = 3$.

apoptosis in response to treatment with the dual inhibitors (35). All three inhibitors inhibited cell proliferation in all cell lines tested (Figs. 5*A* and 5*B* and Fig. S2*C*), but a PIK3CB-selective compound, TGX-221, had little effect on cell proliferation at concentrations up to 10 μM (Fig. S2*D*). In the murine and human OS cell lines, the IC$_{50}$s of GSK2126458 and PIK75 ranged from 7 to 169 nM, similar to the IC$_{50}$ observed in the MCF7 cells, demonstrating the sensitivity of OS cell lines to inhibition of PIK3CA or PI3K/mTOR. PIK75 and GSK2126458 readily induced apoptosis with treatment as shown by caspase 3/7 activation (Fig. S2*E*) and poly(ADP-ribose) polymerase (PARP) cleavage (Fig. 5*C*, assessed only for PIK75). Growth inhibition and apoptosis were seen at drug levels at which phosphorylated AKT (Ser473) and, in the case of GSK2126458, phosphorylated S6 (Ser235/236) levels were reduced (Fig. 5*C* and Fig. S2*F*). The IC$_{50}$ of BEZ235 was 8–51 nM in human cell lines and 178 nM to 1.2 μM in murine cell lines. BEZ235 appeared to cause cytostatic cell growth and did not induce caspase 3/7 activation or PARP cleavage in OS cell lines (Fig. 5*C* and Fig. S2*E*). These data are consistent with a recent study that reports the anti-proliferative and antitumor effects of BEZ235 on OS cell lines (36).

Discussion
Although none of the patients included in this study had documented Li Fraumeni syndrome, rare nonsilent mutations were

present in *TP53* in 12% cases. In previous studies, germline mutations in *TP53* were present in fewer than 3% of patients with OS without a history suggestive of Li Fraumeni syndrome (4). The higher rate of germline mutations detected in this study may be due to or attributable to the nature of the patient population, with a large number of patients from Brazil, where there is a 0.3% population incidence of the p.R337H mutation (37). In our study, 39 of 59 patients were from Brazil and 6 patients had germline *TP53* mutations (15% of Brazilian patients), and 3 of these patients harbored the p.R337H mutation (8% of Brazilian patients). Another possible explanation is the improved ability to detect *TP53* mutations using modern techniques compared with previously used techniques. If these results are confirmed in other study populations, patients with sporadic OS should be referred to a genetic counselor for discussion of testing for Li Fraumeni syndrome, which would constitute a change in clinical practice.

We found four rare nonsilent nucleotide variants in *SQSTM1*, three of which were identical: p.K238E is a SNP (rs11548633) in the TRAF6 binding domain with a minor allele frequency of 0.003 (National Heart, Lung, and Blood Institute Exome Variant Server). Because of the small study size, strong statistical conclusions regarding the association between the *SQSTM1* p.K238E SNP and OS are not possible. The relationship between *SQSTM1* SNPs and OS
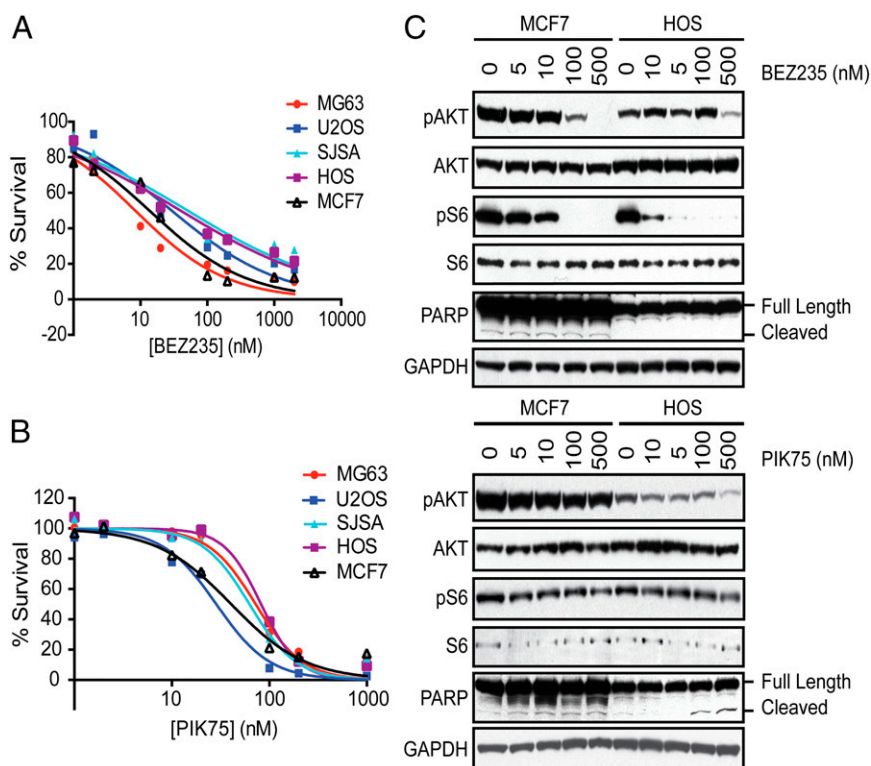
Fig. 5. Small-molecule inhibitors of PI3K/mTOR inhibit osteosarcoma proliferation. Human OS cell lines (MG63, U2OS, SJSA, and HOS) and MCF7 cells (breast cancer cell line with an activating mutation in *PIK3CA*) were treated with (*A*) BEZ235 or (*B*) PIK75 or DMSO (control) for 24 h and viability was assessed with CellTiter-Glo. Experiments were conducted with eight replicates and displayed results are representative of three independent experiments. (*C*) Cells were treated with BEZ235 and PIK75 for 4 h and the effects on the PI3K/mTOR pathway were assessed. Cell extracts were analyzed by Western blotting with antibodies against phosphorylated AKT (Ser473), AKT, phosphorylated S6 (Ser235/236), S6, PARP, and GAPDH (loading control).

should be evaluated using methodologies more suited to identifying germline associations, such as genome-wide association studies.

In the context of pediatric cancers, OS is unique with regards to the somatic mutation rate and the somatic rearrangement rate (26). Pediatric cancers, such as retinoblastoma and rhabdoid tumor, both aggressive malignancies occurring in very young children, have extremely low somatic mutation frequencies. Even those pediatric cancers with higher somatic mutation frequencies, such as neuroblastoma and medulloblastoma, have ~0.4–0.5 mutations per megabase (26). In contrast to these tumor types, the median somatic nonsilent mutation frequency in OS was much higher at 1.2 mutations per megabase. This frequency approaches the median somatic mutation frequency of 1.5 mutations per megabase found in a study of 3,083 tumors of 27 different types, including both childhood and adult cancers (26). This finding suggests an alternative mechanism of transformation in OS tumors compared with other common childhood tumors.

We observed kataegis in 11 of 13 (85%) WGS samples, which is higher than the prevalence of kataegis reported in another cohort of OS samples (50%) (13). Both cohorts are small and so the true prevalence of kataegis remains to be determined once a larger cohort of samples has been analyzed. Similarly, sequencing depth and purity decrease the sensitivity for detecting alterations, so it is possible that we are underestimating the frequency of mutations and structural alterations, and thus kataegis, in OS. In their study of breast cancers, Nik-Zainal et al. (19) suggested that APOBEC1 and APOBEC3s cytidine deaminases may be responsible for the kataegis phenomenon. Because our results and others point to kataegis as a mutational mechanism in OS, we suggest further investigation of the role of APOBEC enzymes in this tumor type.

Complex chains of rearrangements were present in 92% of the OS tumors studied and we observed a median of 230 rearrangements per OS genome, which is higher than previously suggested (15). Although direct comparison of the number and complexity of the rearrangements seen in OS to other pediatric cancers is not possible, OS appear to have a much greater frequency and complexity of structural variations (38). The frequent inactivation of *TP53* may play a role in structural instability in OS, as has been reported in medulloblastoma (39). However, whether genomic instability is simply a byproduct of TP53 inactivation or is, in and of itself, a mechanism of osteosarcomagenesis remains to be answered. In summary, OS is one of the only cancers identified to date that occurs in younger patients in a site not exposed to carcinogens that has a relatively high somatic mutation rate and a very high rate and degree of complexity of structural alterations. This makes OS a model tumor in which to identify mechanisms driving processes, such as kataegis and chromoplexy, and the role of these processes in oncogenesis.

This study confirms the importance and prevalence of TP53 and RB1 inactivation by genomic events, which either affect the *TP53* and *RB1* genes directly or which alter TP53/RB1-interacting genes. Seventy-five percent of samples contained at least one somatic event in *TP53*, which is higher than the 40% previously reported in studies using candidate gene methods (5, 9). We report a slightly lower proportion (75%) of somatic events in *TP53* than the 90% rate reported by Chen et al. in their comprehensive next generation sequencing study (13). This result is likely a result of lack of detection of structural variations in *TP53* in our study, because only 22% of tumors were subjected to WGS. *MDM2* amplification was seen in only 5% of tumors, less often than the 25% frequency previously reported (5, 8, 9, 40–43). Whereas previous studies have reported lack of overlapping mechanisms of TP53 inactivation,

specifically lack of *MDM2* or *COPS3* amplification in osteosarcomas with *TP53* mutations, 34% of our cases have multiple mechanisms of TP53 inactivation. The analysis of mutations (germline and somatic), copy number changes, and rearrangements of multiple genes in one study also allowed us to determine that 56% of the tumors have both TP53 and RB1 inactivated.

Pathway analysis of mutated genes, clinical interpretation of individual genomes (PHIAL), a comparative oncology approach, and a genomic screen all point to a dependence on PI3K/mTOR pathway activation in OS. To our knowledge, this is the first study to report genomic alterations in PI3K/mTOR pathway members in a significant proportion of OS tumors (24%). *PTEN* deletion has been evaluated in a single study in which 4 of 27 osteosarcomas had biallelic deletion of *PTEN*, a similar rate of occurrence as seen in this study (44). A *PTEN* mutation has been detected in a single canine OS cell line but mutations in *PTEN* have not been previously described in human OS samples (45). One recent study using a sequenom assay identified mutations in *PIK3CA* in 3 of 89 tumors (46). However, the other PI3K/mTOR pathway members (*PDPK1*, *AKT1*, and *EIF4B*) containing somatic mutations in this study have not previously been recognized to harbor alterations in OS. Additionally, the PI3K/mTOR pathway is activated by many receptor tyrosine kinases (RTKs), and the pathway has been recognized as a critical effector of alterations that activate RTKs in cancer (47). PHIAL analysis implicated six alterations in RTKs in eight patients (*PDGFRA*, *PDGFRB*, *JAK1*, *ALK*, *KDR*, and *FGFR4*). These patients may benefit from selective RTK inhibitors, but it also reasons that these tumors may be sensitive to inhibition with PI3K/mTOR inhibitors.

In addition, our in vitro and in vivo shRNA screen data strongly suggest that OS cell line proliferation and tumor formation are dependent on the *Pik3ca* and *Mtor* genes signifying that kinase activity of the PI3K/mTOR pathway is required for OS survival. These data are consistent with an earlier report that used kinome profiling to show that AKT (an intermediary kinase in the PI3K/mTOR pathway) is active in OS and its inhibition blocks cell proliferation (48). Interestingly, genetic ablation of either *Pik3ca* or *Mtor* is sufficient to halt cell proliferation and slow tumor formation. This finding suggests that agents that can inhibit either *Pik3ca* or *Mtor* individually should have a similar effect, but experimental evidence from other tumor types demonstrates that many tumors can acquire resistance to single-target inhibitors (49). Thus, a combination of PI3K and mTOR inhibitors or a dual inhibitor may help overcome feedback loops and pathway cross-talk that can mediate resistance.

The universal sensitivity of both human and murine OS cells demonstrates that mutation of PI3K/mTOR is not necessary to confer sensitivity to PI3K/mTOR inhibitors in OS. Using data from the Cancer Cell Line Encyclopedia, we determined that HOS cells, which harbor an *NF1* deletion, are the only human OS cell line used in these studies with an alteration in a PI3K/mTOR pathway member (50). In the HOS cell line the IC_{50} of BEZ235 was 40 nM, the second highest IC_{50} of the cell lines studied, and the IC_{50} of PIK75 was 82 nM, the highest IC_{50} of the cell lines studied. The presence of an *NF1* deletion does not seem to confer increased sensitivity to PI3K/mTOR inhibitors in this panel of human OS cell lines. However, because all of the human OS cell lines display a high degree of sensitivity to PI3K/mTOR pathway inhibitors, it would be difficult to detect increased sensitivity.

Genomic alterations in PI3K/mTOR pathway members is likely only one way in which the PI3K/mTOR pathway becomes active in OS. p70S6K expression, a measure of pathway activity, is present in 70–80% of OS and the level of expression has been correlated with overall and disease-free survival (51). Activation of PI3K-AKT signaling is downstream of several biological processes involved in OS metastasis, such as c-Met and Ezrin expression (52, 53). Micro-RNA-221, expressed at high levels in

OS targets PTEN, increases cell survival, decreases apoptosis, and induces cisplatin resistance (54). These alternative mechanisms of PI3K/mTOR pathway activation in OS may explain the universal sensitivity to PI3K/mTOR inhibitors observed in human osteosarcoma cell lines. In agreement with our data, the dual PI3K/mTOR inhibitor BEZ235 and the α-selective PI3K inhibitor BYL719 have been shown to induce cell cycle arrest and decrease tumor formation in vivo (36, 55). In addition, in preclinical models, mTOR inhibition potentiates the effect of bisphosphonates and sorafenib, drugs being studied in clinical trials in OS (56–58). Other studies have focused on one gene or small molecule but this work demonstrates the convergence of multiple different approaches in human and mouse on the PI3K/mTOR pathway as a whole. In using an unbiased screen and comprehensive genomic assessment, we strengthen the existing evidence regarding a role for the PI3K/mTOR pathway in OS.

Prior clinical studies of mTOR inhibition in sarcomas and our identification of a range of alterations in the PI3K/mTOR pathway serves as a basis for rational clinical trial design. In a phase II trial of ridaforolimus, a second-generation mTOR inhibitor, two patients with OS had confirmed partial responses and one patient with OS had an unconfirmed partial response. The number of OS patients enrolled in this phase II trial is not reported (54 bone tumor patients were enrolled) and so a response rate cannot be determined (59). Given the promising results seen with mTOR inhibition in tuberous sclerosis-associated subependymal giant-cell astrocytomas and renal angiomyolipoma, one could hypothesize that the two patients with partial responses had tumors harboring *TSC2* mutations (60, 61). In a follow-up phase III study, ridaforolimus was administered as maintenance therapy to patients with advanced sarcomas. Only 69 of the 711 patients enrolled in this phase III trial had bone tumors and consequently, the subgroup analysis of bone tumors does not achieve statistical significance (62). To ensure adequate enrollment of OS patients, future clinical trials of PI3K/mTOR inhibition should be limited to OS patients. Given the frequency and range of PI3K/mTOR pathway alterations identified in this study, patient's tumors should be genotyped and activity of the PI3K/mTOR pathway assessed by additional methods so that clinical responses can be correlated with genotype and pathway activity.

Materials and Methods

Sample Selection and Clinical Data. Samples were contributed by hospitals in Brazil, Spain, Mexico, and the United States. All patients had histopathology confirmed to be OS by a pathologist at the local institution. All patients had consented to protocols approved by the Institutional Review Board at the appropriate institution. All but five tumor specimens sequenced were obtained prechemotherapy from the primary tumor at the time of diagnosis. Two tumor specimens were obtained prechemotherapy from a metastatic tumor at the time of diagnosis. Three tumor specimens were obtained postchemotherapy from a metastatic tumor (SJ02, SJ13, DF01). Survival curves were compared using a log-rank (Mantel-Cox) test. Patients who died from treatment toxicity were censored at the time of death.

WGS, WES, RNA Sequencing, and Analysis. Sequencing data reported in this paper is available via National Center for Biotechnology Information dbGap: phs000699.v1.p1 Osteosarcoma Genomics.

Detailed methods for WGS, WES, and RNAseq and analysis are provided in *SI Materials and Methods*. Human genomics data were used as follows: WES data were used for the detection of variants (germline SNP/Indel, somatic SNV/Indel), copy number changes, purity/ploidy, and clonality analysis. WGS data were used for the validation of somatic variants and copy number variation detected in WES and detection of structural variants. RNAseq data were used for the validation of somatic variants detected in WES, analysis of gene expression levels, and detection of gene fusions.

Evaluation for Known Mechanisms of *TP53* and *RB1* Inactivation and for Alterations in Known TP53 and RB1 Interacting Genes. A sample was classified as having TP53, RB1, or CDKN2A/B, deletion if GISTIC2 score for

the gene was −1 or −2 (focal) and COPS3 or MDM2 amplification if GISTIC2 score for the gene was positive, 2 or 1 (Dataset S14). Both WGS and RNASeq data were examined for evidence of TP53 or RB1 rearrangements.

Murine Osteosarcoma. Murine OS spontaneously arising in a mouse model based on conditional deletion of *Tp53* and *Rb1* restricted to the preosteoblast were obtained by killing the animal once a visible tumor causing symptoms was present (32). Tumors were dissected free of normal tissue and frozen at −80 °C. Murine OS cell lines were derived by mincing fresh tumors and culturing in αMEM.

shRNA Constructs and Lentivirus. Lentiviral shRNAs were obtained from The RNAi Consortium (TRC) collection of the Broad Institute (www.broad-institute.org/rnai/public). shRNAs were expressed from the lentiviral expression plasmid pLKO.1. Virus was produced as previously described (63, 64). The TRC numbers for the shRNAs used in the in vitro and in vivo pooled shRNA screens are listed in Datasets S10 and S15, respectively. For individual testing of shRNAs, the TRC numbers are: *Luciferase*, TRCN0000072261; *Pik3ca*, TRCN0000025615; *Pik3cb*, TRCN0000024792. Detailed methods for in vitro and in vivo screening and analysis are provided in *SI Materials and Methods*.

PI3K/mTOR Inhibitor Studies. All inhibitors used in this study were purchased from Selleck Chemicals. Human OS cell lines were obtained from ATCC. Human OS cell lines were cultured with drug or DMSO control for 24 h and viability was assessed with the CellTiter-Glo luminescent cell viability assay (Promega). Murine OS cell lines were cultured with drug or control for 72 h and viability was assessed with the cell proliferation reagent WST-1 (Roche). Caspase 3/7 activation after 16 h of treatment with inhibitors was determined with the Caspase-Glo 3/7 luminescence assay (Promega). For Western blot analysis, human OS cell lines were treated with inhibitors for 4 h; murine OS cell lines were treated for 24 h. Western blotting was performed as previously described (65). All primary antibodies were purchased from Cell Signaling. HRP-conjugated secondary antibodies were from Jackson Laboratories.

1. Siegel R, Naishadham D, Jemal A (2013) Cancer statistics, 2013. *CA Cancer J Clin* 63(1): 11–30.
2. Mirabello L, Troisi RJ, Savage SA (2009) Osteosarcoma incidence and survival rates from 1973 to 2004: Data from the Surveillance, Epidemiology, and End Results Program. *Cancer* 115(7):1531–1543.
3. Hansen MF, et al. (1985) Osteosarcoma and retinoblastoma: A shared chromosomal mechanism revealing recessive predisposition. *Proc Natl Acad Sci USA* 82(18): 6216–6220.
4. McIntyre JF, et al. (1994) Germline mutations of the p53 tumor suppressor gene in children with osteosarcoma. *J Clin Oncol* 12(5):925–930.
5. Kansara M, Thomas DM (2007) Molecular pathogenesis of osteosarcoma. *DNA Cell Biol* 26(1):1–18.
6. Ralston SH, Albagha OM (2011) Genetic determinants of Paget's disease of bone. *Ann N Y Acad Sci* 1240:53–60.
7. Savage SA, et al. (2013) Genome-wide association study identifies two susceptibility loci for osteosarcoma. *Nat Genet* 45(7):799–803.
8. Henriksen J, et al. (2003) Amplification and overexpression of COPS3 in osteosarcomas potentially target TP53 for proteasome-mediated degradation. *Oncogene* 22(34): 5358–5361.
9. Miller CW, et al. (1996) Alterations of the p53, Rb and MDM2 genes in osteosarcoma. *J Cancer Res Clin Oncol* 122(9):559–565.
10. Wadayama B, et al. (1994) Mutation spectrum of the retinoblastoma gene in osteosarcomas. *Cancer Res* 54(11):3042–3048.
11. Toguchida J, et al. (1988) Chromosomal reorganization for the expression of recessive mutation of retinoblastoma susceptibility gene in the development of osteosarcoma. *Cancer Res* 48(14):3939–3943.
12. Tsuchiya T, et al. (2000) Analysis of the p16INK4, p14ARF, p15, TP53, and MDM2 genes and their prognostic implications in osteosarcoma and Ewing sarcoma. *Cancer Genet Cytogenet* 120(2):91–98.
13. Chen X, et al.; St. Jude Children's Research Hospital–Washington University Pediatric Cancer Genome Project (2014) Recurrent somatic structural variations contribute to tumorigenesis in pediatric osteosarcoma. *Cell Reports* 7(1):104–112.
14. Helman LJ, Meltzer P (2003) Mechanisms of sarcoma development. *Nat Rev Cancer* 3(9):685–694.
15. Stephens PJ, et al. (2011) Massive genomic rearrangement acquired in a single catastrophic event during cancer development. *Cell* 144(1):27–40.
16. Cibulskis K, et al. (2013) Sensitive detection of somatic point mutations in impure and heterogeneous cancer samples. *Nat Biotechnol* 31(3):213–219.
17. Adzhubei IA, et al. (2010) A method and server for predicting damaging missense mutations. *Nat Methods* 7(4):248–249.
18. Rea SL, Walsh JP, Layfield R, Ratajczak T, Xu J (2013) New insights into the role of sequestosome 1/p62 mutant proteins in the pathogenesis of Paget's disease of bone. *Endocr Rev* 34(4):501–524.
19. Nik-Zainal S, et al.; Breast Cancer Working Group of the International Cancer Genome Consortium (2012) Mutational processes molding the genomes of 21 breast cancers. *Cell* 149(5):979–993.
20. Kostic AD, et al. (2011) PathSeq: Software to identify or discover microbes by deep sequencing of human tissue. *Nat Biotechnol* 29(5):393–396.
21. Mermel CH, et al. (2011) GISTIC2.0 facilitates sensitive and confident localization of the targets of focal somatic copy-number alteration in human cancers. *Genome Biol* 12(4):R41.
22. Mejia-Guerrero S, et al. (2010) Characterization of the 12q15 MDM2 and 12q13-14 CDK4 amplicons and clinical correlations in osteosarcoma. *Genes Chromosomes Cancer* 49(6):518–525.
23. Drier Y, et al. (2013) Somatic rearrangements across cancer reveal classes of samples with distinct patterns of DNA breakage and rearrangement-induced hypermutability. *Genome Res* 23(2):228–235.
24. Baca SC, et al. (2013) Punctuated evolution of prostate cancer genomes. *Cell* 153(3): 666–677.
25. Shen MM (2013) Chromoplexy: A new category of complex rearrangements in the cancer genome. *Cancer Cell* 23(5):567–569.
26. Lawrence MS, et al. (2013) Mutational heterogeneity in cancer and the search for new cancer-associated genes. *Nature* 499(7457):214–218.
27. Forbes SA, et al. (2014) COSMIC: exploring the world's knowledge of somatic mutations in human cancer. *Nucleic Acids Res*, 10.1093/nar/gku1075. Available at cancer. sanger.ac.uk.
28. Lohr JG, et al. (2012) Discovery and prioritization of somatic mutations in diffuse large B-cell lymphoma (DLBCL) by whole-exome sequencing. *Proc Natl Acad Sci USA* 109(10):3879–3884.
29. Subramanian A, et al. (2005) Gene set enrichment analysis: A knowledge-based approach for interpreting genome-wide expression profiles. *Proc Natl Acad Sci USA* 102(43):15545–15550.
30. Van Allen EM, et al. (2014) Whole-exome sequencing and clinical interpretation of formalin-fixed, paraffin-embedded tumor samples to guide precision cancer medicine. *Nat Med* 20(6):682–688.
31. Adzhubei I, Jordan DM, Sunyaev SR (2013) Predicting functional effect of human missense mutations using PolyPhen-2. *Curr Protoc Hum Genet*, Chapter 7:Unit 7.20.
32. Walkley CR, et al. (2008) Conditional mouse osteosarcoma, dependent on p53 loss and potentiated by loss of Rb, mimics the human disease. *Genes Dev* 22(12): 1662–1676.
33. Cheung LW, et al. (2011) High frequency of PIK3R1 and PIK3R2 mutations in endometrial cancer elucidates a novel mechanism for regulation of PTEN protein stability. *Cancer Discov* 1(2):170–185.
34. Allan EH, et al. (2003) Differentiation potential of a mouse bone marrow stromal cell line. *J Cell Biochem* 90(1):158–169.
35. Leung E, Kim JE, Rewcastle GW, Finlay GJ, Baguley BC (2011) Comparison of the effects of the PI3K/mTOR inhibitors NVP-BEZ235 and GSK2126458 on tamoxifen-resistant breast cancer cells. *Cancer Biol Ther* 11(11):938–946.
36. Gobin B, et al. (2014) NVP-BEZ235, a dual PI3K/mTOR inhibitor, inhibits osteosarcoma cell proliferation and tumor development in vivo with an improved survival rate. *Cancer Lett* 344(2):291–298.
37. Seidinger AL, et al. (2011) Association of the highly prevalent TP53 R337H mutation with pediatric choroid plexus carcinoma and osteosarcoma in southeast Brazil. *Cancer* 117(10):2228–2235.
38. Zhang J, et al. (2012) The genetic basis of early T-cell precursor acute lymphoblastic leukaemia. *Nature* 481(7380):157–163.
39. Rausch T, et al. (2012) Genome sequencing of pediatric medulloblastoma links catastrophic DNA rearrangements with TP53 mutations. *Cell* 148(1-2):59–71.
40. Oliner JD, Kinzler KW, Meltzer PS, George DL, Vogelstein B (1992) Amplification of a gene encoding a p53-associated protein in human sarcomas. *Nature* 358(6381):80–83.
41. Lonardo F, Ueda T, Huvos AG, Healey J, Ladanyi M (1997) p53 and MDM2 alterations in osteosarcomas: Correlation with clinicopathologic features and proliferative rate. *Cancer* 79(8):1541–1547.
42. Ladanyi M, et al. (1993) MDM2 gene amplification in metastatic osteosarcoma. *Cancer Res* 53(1):16–18.
43. Yan T, et al. (2007) COPS3 amplification and clinical outcome in osteosarcoma. *Cancer* 109(9):1870–1876.
44. Freeman SS, et al. (2008) Copy number gains in EGFR and copy number losses in PTEN are common events in osteosarcoma tumors. *Cancer* 113(6):1453–1461.
45. Levine RA, Forest T, Smith C (2002) Tumor suppressor PTEN is mutated in canine osteosarcoma cell lines and tumors. *Vet Pathol* 39(3):372–378.
46. Choy E, et al. (2012) High-throughput genotyping in osteosarcoma identifies multiple mutations in phosphoinositide-3-kinase and other oncogenes. *Cancer* 118(11): 2905–2914.
47. Engelman JA (2009) Targeting PI3K signalling in cancer: Opportunities, challenges and limitations. *Nat Rev Cancer* 9(8):550–562.

48. Kuijjer ML, et al. (2014) Kinome and mRNA expression profiling of high-grade osteosarcoma cell lines implies Akt signaling as possible target for therapy. *BMC Med Genomics* 7:4.

49. Kwong LN, Davies MA (2013) Navigating the therapeutic complexity of PI3K pathway inhibition in melanoma. *Clin Cancer Res* 19(19):5310–5319.

50. Barretina J, et al. (2012) The Cancer Cell Line Encyclopedia enables predictive modelling of anticancer drug sensitivity. *Nature* 483(7391):603–607.

51. Zhou Q, et al. (2010) mTOR/p70S6K signal transduction pathway contributes to osteosarcoma progression and patients' prognosis. *Med Oncol* 27(4):1239–1245.

52. Wan X, Mendoza A, Khanna C, Helman LJ (2005) Rapamycin inhibits ezrin-mediated metastatic behavior in a murine model of osteosarcoma. *Cancer Res* 65(6):2406–2411.

53. Wang K, Zhuang Y, Liu C, Li Y (2012) Inhibition of c-Met activation sensitizes osteosarcoma cells to cisplatin via suppression of the PI3K-Akt signaling. *Arch Biochem Biophys* 526(1):38–43.

54. Zhao G, et al. (2013) MicroRNA-221 induces cell survival and cisplatin resistance through PI3K/Akt pathway in human osteosarcoma. *PLoS ONE* 8(1):e53906.

55. Gobin B, et al. (2014) BYL719, a new α-specific PI3K inhibitor: Single administration and in combination with conventional chemotherapy for the treatment of osteosarcoma. *Int J Cancer*, 10.1002/ijc.29040.

56. Pignochino Y, et al. (2013) The combination of sorafenib and everolimus abrogates mTORC1 and mTORC2 upregulation in osteosarcoma preclinical models. *Clin Cancer Res* 19(8):2117–2131.

57. Moriceau G, et al. (2010) Zoledronic acid potentiates mTOR inhibition and abolishes the resistance of osteosarcoma cells to RAD001 (everolimus): Pivotal role of the prenylation process. *Cancer Res* 70(24):10329–10339.

58. Tsubaki M, et al. (2012) Reduction of metastasis, cell invasion, and adhesion in mouse osteosarcoma by YM529/ONO-5920-induced blockade of the Ras/MEK/ERK and Ras/PI3K/Akt pathway. *Toxicol Appl Pharmacol* 259(3):402–410.

59. Chawla SP, et al. (2012) Phase II study of the mammalian target of rapamycin inhibitor ridaforolimus in patients with advanced bone and soft tissue sarcomas. *J Clin Oncol* 30(1):78–84.

60. Bissler JJ, et al. (2013) Everolimus for angiomyolipoma associated with tuberous sclerosis complex or sporadic lymphangioleiomyomatosis (EXIST-2): A multicentre, randomised, double-blind, placebo-controlled trial. *Lancet* 381(9869):817–824.

61. Franz DN, et al. (2013) Efficacy and safety of everolimus for subependymal giant cell astrocytomas associated with tuberous sclerosis complex (EXIST-1): A multicentre, randomised, placebo-controlled phase 3 trial. *Lancet* 381(9861):125–132.

62. Demetri GD, et al. (2013) Results of an international randomized phase III trial of the mammalian target of rapamycin inhibitor ridaforolimus versus placebo to control metastatic sarcomas in patients after benefit from prior chemotherapy. *J Clin Oncol* 31(19):2485–2492.

63. Luo B, et al. (2008) Highly parallel identification of essential genes in cancer cells. *Proc Natl Acad Sci USA* 105(51):20380–20385.

64. Whittaker SR, et al. (2013) A genome-scale RNA interference screen implicates NF1 loss in resistance to RAF inhibition. *Cancer Discov* 3(3):350–362.

65. Janeway KA, et al. (2007) Pediatric KIT wild-type and platelet-derived growth factor receptor alpha-wild-type gastrointestinal stromal tumors share KIT activation but not mechanisms of genetic progression with adult gastrointestinal stromal tumors. *Cancer Res* 67(19):9084–9088.